Meteoritics & Planetary Science 40, Nr 9/10, 1353–1361 (2005)
Abstract available online at http://meteoritics.org

Experimental reproduction of tectonic deformation lamellae in quartz and comparison to shock-induced planar deformation features

M. G. C. VERNOOIJ[1, 2] and F. LANGENHORST[2, 3*]

[1]Geologisches Institut, ETH Zürich, Sonneggstrasse 5, 8092 Zürich, Switzerland
[2]Bayerisches Geoinstitut, Universität Bayreuth, D-95440 Bayreuth, Germany
[3]Institut für Geowissenschaften, Friedrich-Schiller-Universität Jena, Burgweg 11, D-07749 Jena, Germany
*Corresponding author. E-mail: Falko.Langenhorst@uni-jena.de

(Received 25 April 2005; revision accepted 06 June 2005)

Abstract–Planar features can develop in quartz during comparatively slow tectonic deformation and during very fast dynamic shock metamorphism. Despite their very different structural nature, tectonically induced deformation lamellae have sometimes been mistaken as shock-induced planar deformation features (PDFs). To understand the formation of deformation lamellae and to address the substantial differences between them and PDFs, we have conducted deformation experiments on single crystals of quartz in a Griggs-type apparatus, at a temperature of 800 °C, a confining pressure of 12 kbar, and a strain rate of $0.7–1.1 \cdot 10^{-6}$. The deformed samples were analyzed with transmission electron microscopy (TEM) and compared to natural PDFs from the Ries Crater, Germany. TEM revealed that tectonic deformation lamellae are associated with numerous sub-parallel curved subgrain walls, across which the orientation of the crystal changes slightly. The formation of deformation lamellae is due to glide- and climb-controlled deformation in the exponential creep regime. In contrast, the PDFs in shocked quartz from the Ries are perfectly planar, crystallographically controlled features that originally represented amorphous lamellae. Due to post-shock annealing and hydrothermal activity they are recrystallized and decorated with fluid inclusions.

INTRODUCTION

The detection of shock metamorphism in minerals provides unequivocal proof for the recognition of impact structures and their related distal or global ejecta. Quartz is the prime mineral indicator of impact deformation, due to its large variety of shock effects and its widespread occurrence as a rock-forming mineral (Stöffler and Langenhorst 1994; Grieve et al. 1996; French 1998). Shock effects in quartz range from the formation of mechanical Brazil twins, planar deformation features (PDFs), diaplectic glass, lechatelierite, to high-pressure polymorphs (coesite, stishovite, and post-stishovite phases) (see, e.g., Langenhorst et al. 1992; Leroux et al. 1994; Stöffler and Langenhorst 1994; Langenhorst and Deutsch 1998; Sharp et al. 1999). PDFs in quartz occur as single or multiple sets of parallel, planar lamellae that are generated at shock pressures ≥10–15 GPa and are usually oriented parallel to rhombohedral planes (Doukhan 1995). They are the most robust shock indicators in many important rock-forming silicate minerals because they are often preserved as last evidence for an impact event despite long-standing annealing and alteration.

Under the optical microscope, deformation lamellae in quartz from tectonically deformed crustal rocks sometimes seem to resemble PDFs, although their origin is completely different. Deformation lamellae are narrow planar features that result from slow tectonic deformation. They seem to be aligned along crystallographic planes (Böhm 1882; Becke 1893; Christie and Raleigh 1959) and can also be decorated with fluid inclusions. The apparent optical resemblance between deformation lamellae and PDFs has led to misidentifications of impact craters and distal ejecta layers such as the Susice, Sevetin, and Azuara structures, and the Permo-Triassic boundary layer (Cordier et al. 1994; Mossman et al. 1998; Langenhorst and Deutsch 1996; Langenhorst 2002; Langenhorst et al. 2005).

Previous TEM studies have revealed a broad spectrum of microstructures that can be assigned to the optically visible deformation lamellae. In experimentally deformed quartz, lamellae are ascribed to walls of tangled dislocations (McLaren et al. 1970) and even zones of glass were reported (Christie and Ardell 1974). Natural deformation lamellae were attributed to elongated subgrains, subgrain walls, and zones of different dislocation density and water bubble content (McLaren and Hobbs 1972; White 1973; Christie and Ardell 1976; Drury 1993).

In this paper, we demonstrate the experimental reproduction of extensive deformation lamellae during slow ductile deformation of single crystals of quartz in the presence of water. The optically visible features are directly correlated to the defect microstructure in order to better understand the formation mechanism and orientation of deformation lamellae and to address the fundamental optical and microstructural differences between the experimentally produced tectonic deformation lamellae and natural shock-induced PDFs. It is hoped that our observations will help to improve the optical discrimination between deformation lamellae and PDFs in quartz.

SAMPLES AND METHODS

Griggs Rig Deformation Experiments

For deformation experiments, a natural single crystal of quartz from Arizona with well-developed crystal faces and free of inclusions was cut and cored in various orientations into sample cylinders (Table 1). The cylindrical samples, 11.5 ± 0.5 mm long and 5.8 mm in diameter, were weld-sealed into gold jackets (400 µm wall thickness) with 1 vol% of distilled water.

The experiments were performed in a Tullis-modified Griggs apparatus (Tullis and Tullis 1986) with NaCl as a solid medium. The sample assembly is shown in Fig. 1. Deformation experiments were carried out in the ductile deformation regime with a confining pressure of 11–12 kbar and at a temperature of 800 °C in uniaxial compression at a strain rate of $0.7–1.1 \cdot 10^{-6}$ s^{-1} (Table 1). The temperature was applied with a graphite resistance furnace and was measured with two Pt-Pt10%Rh thermocouples. The temperature gradients were minimized by enclosing the sample in a Ni tube (700 µm wall thickness).

The sample was brought to experimental conditions in 6–8 hr. Pressure and temperature were raised simultaneously, following the water isochore of $1\ g \cdot cm^{-3}$ as closely as possible; this path is described by Den Brok (1992). To equilibrate the experimental conditions, each sample was held at experimental pressure and temperature for 16–19 hours prior to deformation. After deformation, pressure and temperature were lowered in ~1 hour, again following the water isochore of $1\ g \cdot cm^{-3}$.

The measured axial displacement and load were corrected for apparatus distortion (at 800 °C and 12 kbar) and for friction, respectively. Differential stresses were calculated using the initial cross-section of the samples. Finite strain was calculated with respect to the sample length at room temperature and pressure.

PDF-Bearing Quartz Grains from Ries Suevite

For comparative study, shocked quartz grains from the Ries crater in Germany were prepared. We particularly searched for quartz grains containing PDFs that are decorated with water bubbles as do some of the experimentally produced deformation lamellae. Such grains were found in the clastic matrix of suevites from the Aumühle and Seelbronn quarries and the Zipplingen outcrop. At these localities the so-called fall-out suevite occurs, which is mostly derived from crystalline basement rocks (Stöffler and Ostertag 1983). The quartz grains reflect shock stage Ib (20–35 GPa) according to the classification of progressive shock metamorphism (Stöffler 1971).

Optical and Transmission Electron Microscopy

The optical microphotographs were taken from 30 µm petrographic thin sections under crossed polarizers. Orientations of the lamellae were measured with a four-axis Leitz universal stage mounted on a Leitz Orthoplan microscope. For TEM examination, selected areas of the thin sections with either experimental deformation lamellae or natural shock-induced PDFs in quartz were glued onto copper grids. These samples were then thinned by ion milling in a Gatan Duomill until electron transparency was reached (<0.1–0.2 µm). Specimens were finally coated with carbon to avoid charge problems. The TEM investigations were performed with a Philips field emission gun (FEG) CM20 transmission electron microscope (TEM) at the Bayerisches Geoinstitut, operating at 200 kV. Conventional bright-field and dark-field imaging techniques were used to observe and characterize the microstructures in quartz.

RESULTS

Experimentally Produced Deformation Lamellae in Quartz

Under the optical microscope, the experimentally produced deformation lamellae are recognizable as sub-parallel, >1 µm wide bands, across which the birefringence alternately changes (Figs. 2a and 2b), as described by Christie and Raleigh (1959). The bands are not strictly planar and their spacing decreases with increasing differential stress from ~4 µm at ~100 MPa to ~2 µm at ~400 MPa. Thicker lamellae often tend to branch into thinner lamellae (Fig. 2a). When they are decorated with fluid inclusions, deformation lamellae are of the Böhm type (Fig. 2c). Especially these kinds of deformation lamellae show some optical similarity to shock-induced decorated PDFs.

Overall, deformation lamellae were observed in samples that were deformed to low finite strains (≤26%) with the following crystallographic orientations (listed according to increasing abundance): compression axis σ_1 (i) parallel to the *c* axis (GRZ25), (ii) at 45° to the *c* and *a* axes (GRZ16 and GRZ17), and (iii) at 45° to the *c* axis and *m* plane (GRZ28), i.e., $(10\bar{1}0)$ (Table 1). In GRZ28 deformed to a finite strain of 2.8%,

Table 1. Summary of experimental data. P_c, confining pressure; t_1, elapsed time to reach PT conditions; t_2 time at PT conditions before deformation; t_3, elapsed time after deformation to reach room PT conditions.

Sample number	Water (vol%)	Starting orientation (σ_1)	Strain rate (s^{-1})	Finite strain (%)	P_c (MPa)	T (°C)	t_1 (h:m)	t_2 (h:m)	t_3 (h:m)	Yield stress (MPa)	Deformation lamellae (orientation)	Appearance
GRZ16	1	45° to *c* and *a*	$0.7 \cdot 10^{-6}$	11	1200	800	07:54	16:24	01:12	40	~ basal	Isolated patches
GRZ17	1	45° to *c* and *a*	$1.1 \cdot 10^{-6}$	21	1190	800	08:22	15:34	00:58	160	~ basal	Isolated patches
GRZ20	1	45° to *c* and *a*	$1.0 \cdot 10^{-6}$	28	1120	800	05:14	19:12	00:58	60	–	–
GRZ21	1	45° to *c* and *a*	$1.0 \cdot 10^{-6}$	50	1110	800	07:02	14:50	00:53	90	–	–
GRZ22	1	// *a*	$1.0 \cdot 10^{-6}$	32	1240	800	06:55	16:21	01:07	90	–	–
GRZ25	1	// *c*	$1.1 \cdot 10^{-6}$	26	1220	800	07:24	16:48	00:54	405	~rhombohedral ~basal	Isolated patches
GRZ28	1	45° to *c* and $(10\bar{1}0)$	$1.0 \cdot 10^{-6}$	3	1200	800	08:06	20:00	00:48	330	~basal	Continuous

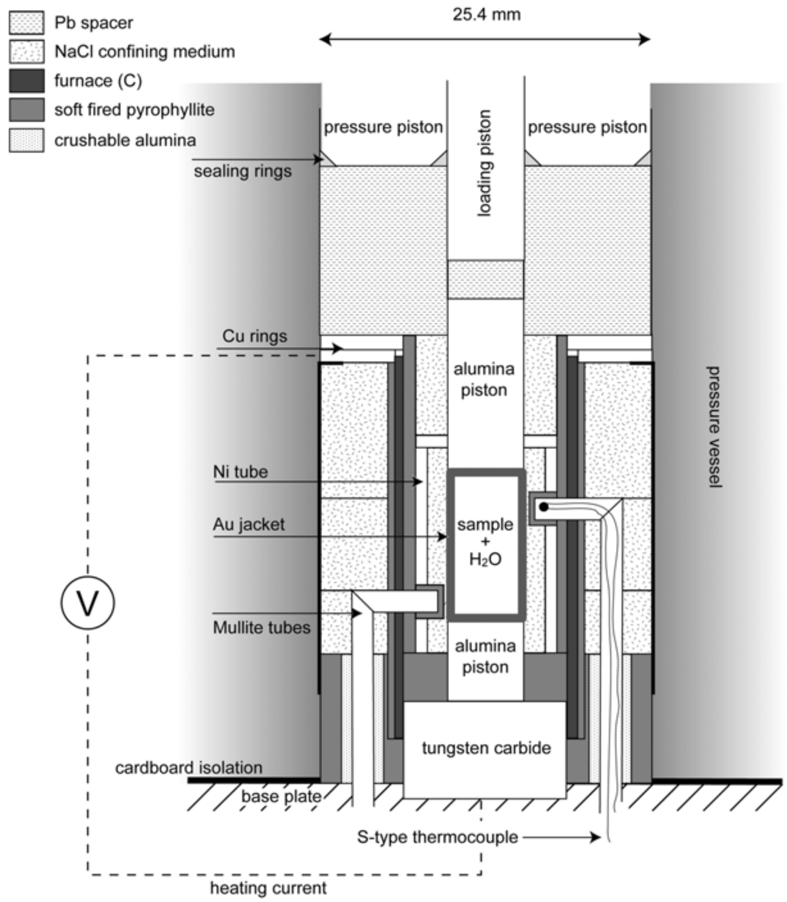

Fig. 1. Sample assembly used in a Tullis-modified Griggs apparatus to deform single crystals of quartz. NaCl was used as a solid medium.

the deformation lamellae are homogeneously spread through one half of the sample, whereas GRZ16, GRZ17 and GRZ25 (11%, 21%, and 26% finite strains) contain deformation lamellae only in single patches distributed throughout the samples. It is remarkable that deformation lamellae are not observed in samples deformed to large strains at 45° to the *c* and *a* axes (GRZ20, GRZ21). Also, compression along the *a* axis did not yield any deformation lamellae.

In most cases, deformation lamellae seem to be roughly parallel to the basal plane (Fig. 2b), as measured by universal stage. In sample GRZ25, which was deformed at high differential stress with the basal plane perpendicular to the compression direction, they are also observed sub-parallel to rhombohedral planes, but exclusively in areas where the *c* axis has not rotated too far away from the compression direction. Deformation lamellae are always associated with larger, ~50 μm wide zones of undulatory extinction, suggesting a gradual misorientation of the deformed crystal. These undulatory zones are always approximately parallel to the *c* direction (Fig. 2b). If the deformation lamellae are bent, the zones of undulatory extinction are also curved.

TEM revealed that the experimentally produced deformation lamellae are associated with slightly curved, non-planar subgrain walls (Figs. 3a and 3b). The subgrain walls are usually composed of one set of straight, well-organized dislocations (Fig. 3a). Free dislocations in the vicinity of the subgrain walls are curved, entangled, and sometimes connected to tiny water bubbles (Fig. 3a), or they form numerous junctions. The subgrain walls themselves are only rarely decorated with fluid inclusions.

Deformed quartz crystals are penetrated by numerous of these aligned subgrain walls, often occurring in pairs (Fig. 4). Changes in electron diffraction contrast across, and fringes at, subgrain walls indicate that the crystal is alternately tilted about the subgrain walls with a misorientation of about 1–3°. It is this alternating orientation which leads to the variation in optical birefringence and the visibility of deformation lamellae at the optical scale. In principle, the lamellae can thus be regarded as strongly elongated subgrains. At the TEM scale it is obvious that a crystallographic orientation of the subgrain walls can not be identified, because they do not define a crystallographic plane and are of a curved nature.

In order to determine the Burgers vectors using the $g \cdot b = 0$ criterion, TEM images were taken with diffraction vectors $g = 10\bar{1}1$ and $g = 0003$. Most dislocations are out of contrast with $g = 0003$ but are well visible with $g = 10\bar{1}1$. Therefore, the Burgers vector of the dislocations is $b = 1/3\langle 11\bar{2}0\rangle$, which is known to be the energetically most favorable

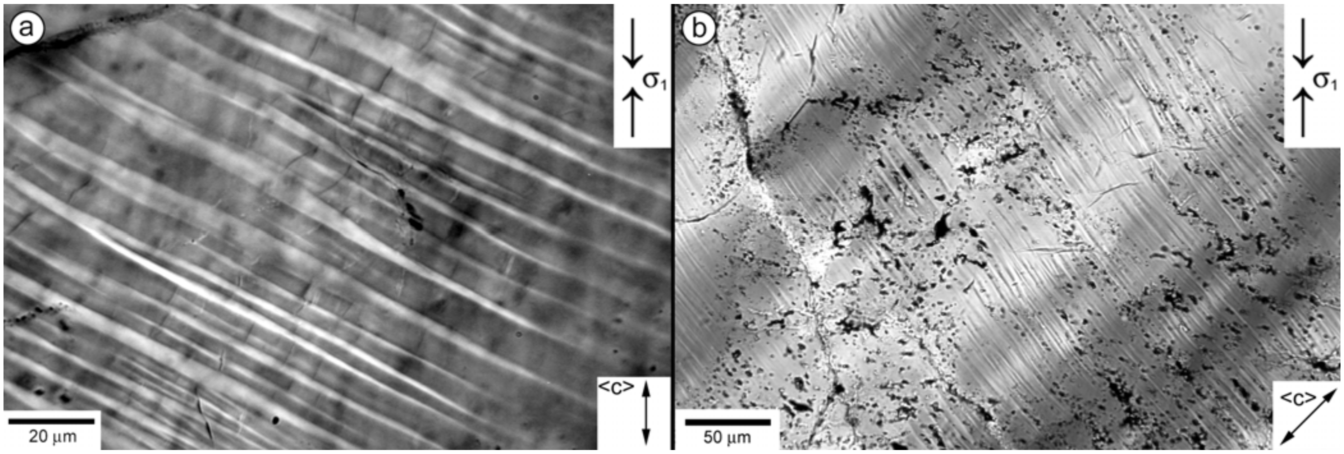

Fig. 2. Optical micrographs in polarized light of experimentally formed deformation lamellae in sample GRZ25 deformed parallel to the *c* axis and in samples (GRZ16 and GRZ28) deformed at 45° to the *c* axis. a) GRZ25, tectonic deformation lamellae are in a sub-parallel, non-planar arrangement. Note that single lamellae sometimes branch into two thinner lamellae. Small unloading fractures are observed between the lamellae. b) GRZ28, deformation lamellae are always associated with undulose zones that are approximately parallel to the *c* axis.

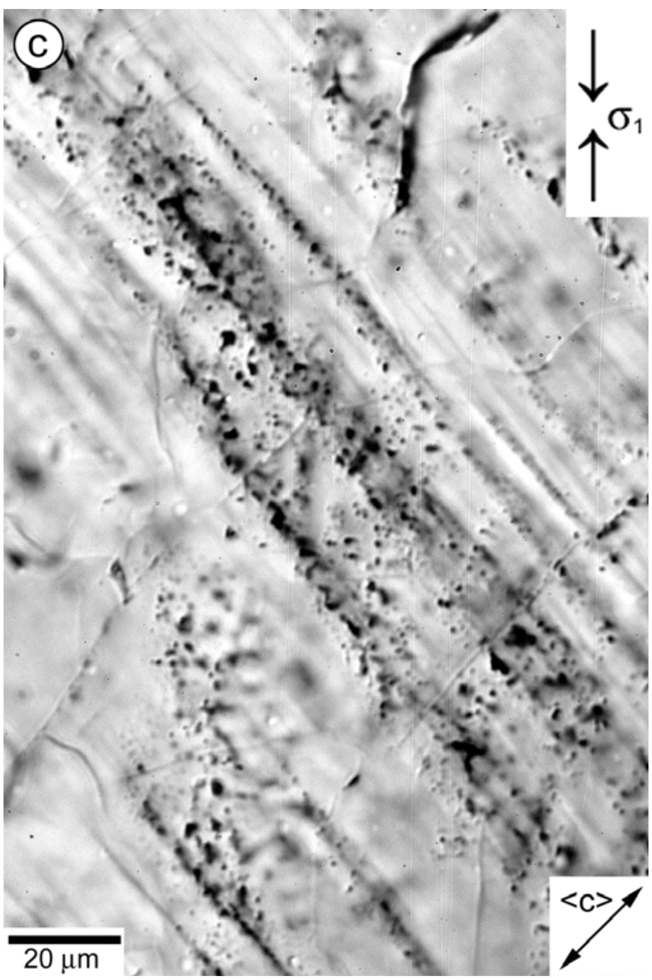

Fig. 2. *Continued.* c) GRZ16, deformation lamellae that are decorated with fluid inclusions show resemblance with shock induced PDFs.

Burgers vector in quartz (Doukhan 1995). The density of these *a* dislocations is on the order of 10^{10} cm^{-2}.

Planar Deformation Features (PDFs) in Shocked Quartz from the Ries Crater

Optically, the decorated type of PDFs in analyzed quartz grains from the Ries crater appear as perfectly planar and parallel elements with a spacing >4 µm (Fig. 5a). TEM analysis revealed that even more closely spaced PDFs exist (<1 µm) that are not resolvable at the optical scale (Fig. 6). There are no orientation changes across the PDFs similar to those observed in case of tectonic deformation lamellae. Under the TEM, PDFs are decorated with fluid inclusions, indicating migration of water during post-shock annealing of suevites. At least three different PDF orientations were induced in the quartz grains (Figs. 5b and 6b). For example, the three different PDF orientations in the quartz grain shown in Fig. 6b belong to two corresponding rhombohedral planes, $(10\bar{1}3)$ and $(\bar{1}013)$, and one prismatic plane, $(10\bar{1}0)$. This combination of rhombohedral and prismatic planes is commonly observed in shocked quartz and indicates a moderate shock pressure of about 20 GPa (Langenhorst and Deutsch 1994).

TEM reveals furthermore that the PDFs in these quartz grains from the Ries crater consist of tiny dislocation loops, voids and bubbles. Similar features have been observed in shocked quartz from other impact sites (Goltrant et al. 1991, 1992; Leroux et al. 1994, 1995) and are attributed to post-shock recrystallization of originally amorphous PDFs. In agreement with these studies, there are only few free dislocations (density $\leq 0.2 \cdot 10^{10}$ cm^{-2}) in the vicinity of the PDFs. This contrasts with the observations on the experimental deformation lamellae, which are associated with

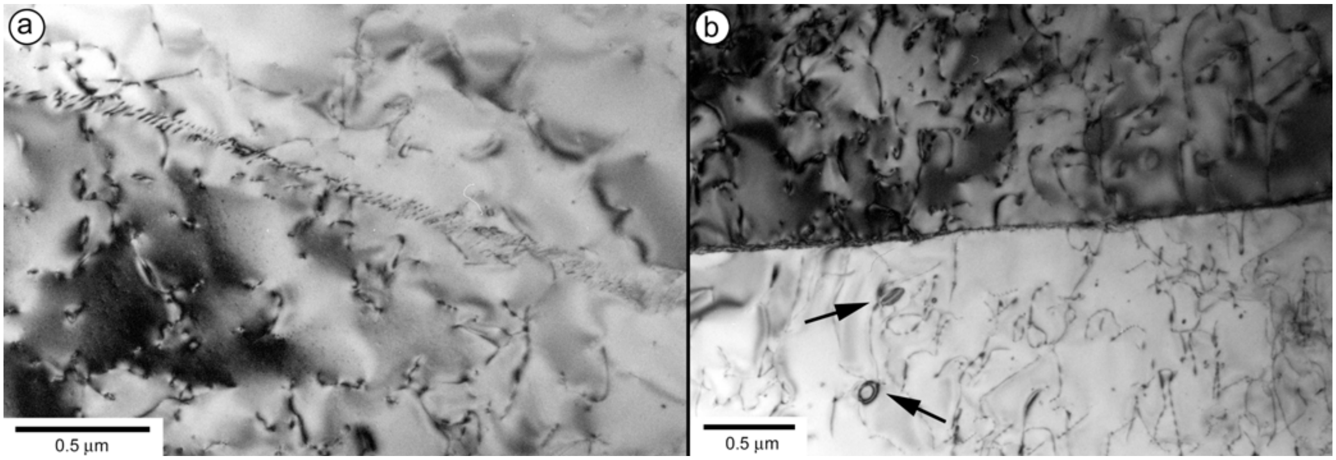

Fig. 3. TEM micrographs, bright field images of subgrain walls in sample (GRZ28) deformed at 45° to the *c* axis and *m* plane. The free dislocations in the vicinity of the walls are curved, entangled and sometimes carry water in tiny inclusions (black arrows). a) The subgrain walls consist of well organized straight dislocations. b) The contrast changes across subgrain walls indicate that the subgrains are slightly tilted.

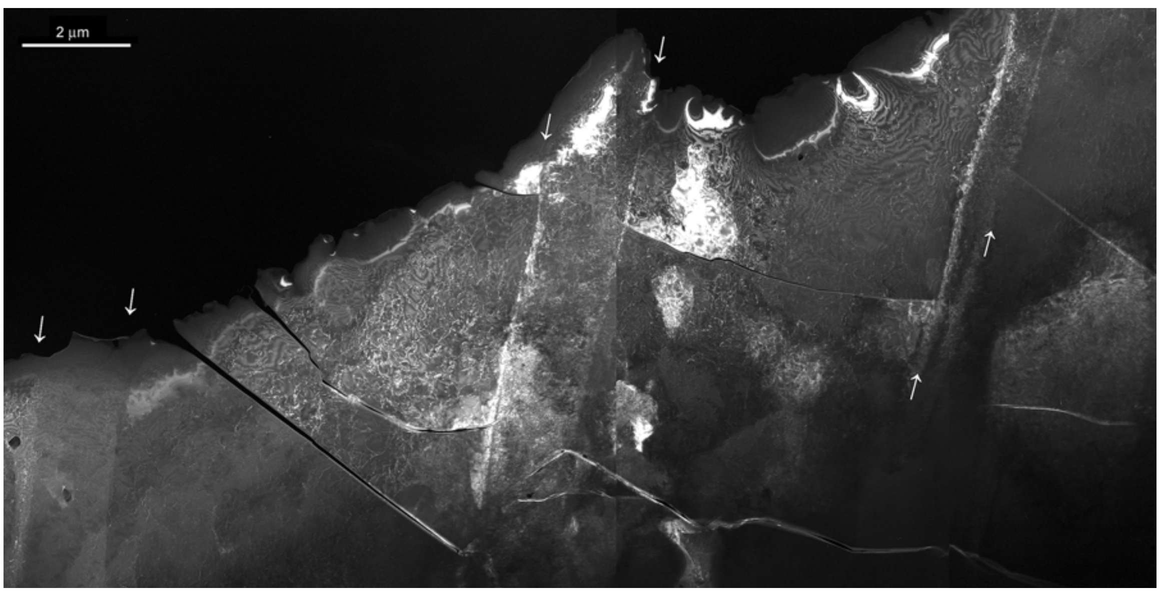

Fig. 4. Dark field weak beam TEM image ($g = 10\bar{1}1$) of sample GRZ25 (deformed parallel to the *c* axis). A set of subgrain walls (white arrows) is visible that is associated with optical deformation lamellae. The subgrain walls are neither perfectly parallel nor perfectly planar and can therefore not be assigned to crystallographic planes. The open cracks are unloading cracks or cracks that are caused by the preparation of the sample.

dislocation densities of 10^{10} cm^{-2}. The free dislocations in shocked quartz may have pre-existed or developed during post-shock annealing and did not play a role in the original shock deformation (Christie and Ardell 1976; Grieve et al. 1996; Langenhorst 2002).

DISCUSSION

Nature and Formation of Deformation Lamellae

In this study, we have experimentally reproduced deformation lamellae in single-crystal quartz that show great similarity to natural deformation lamellae formed in tectonically deformed quartz (e.g., McLaren and Hobbs 1972). Our TEM observations reveal that the optically visible, experimental deformation lamellae represent elongated subgrains, which is in agreement with the microstructural characteristics of deformation lamellae in naturally deformed quartz (McLaren and Hobbs 1972; White 1973; Blenkinsop and Drury 1988). The formation of the subgrains is due to the recovery of dislocations into gently curved subparallel subgrain walls, resulting in a banded substructure that causes an alternating change in optical birefringence. Overall, the presence of subgrain walls and

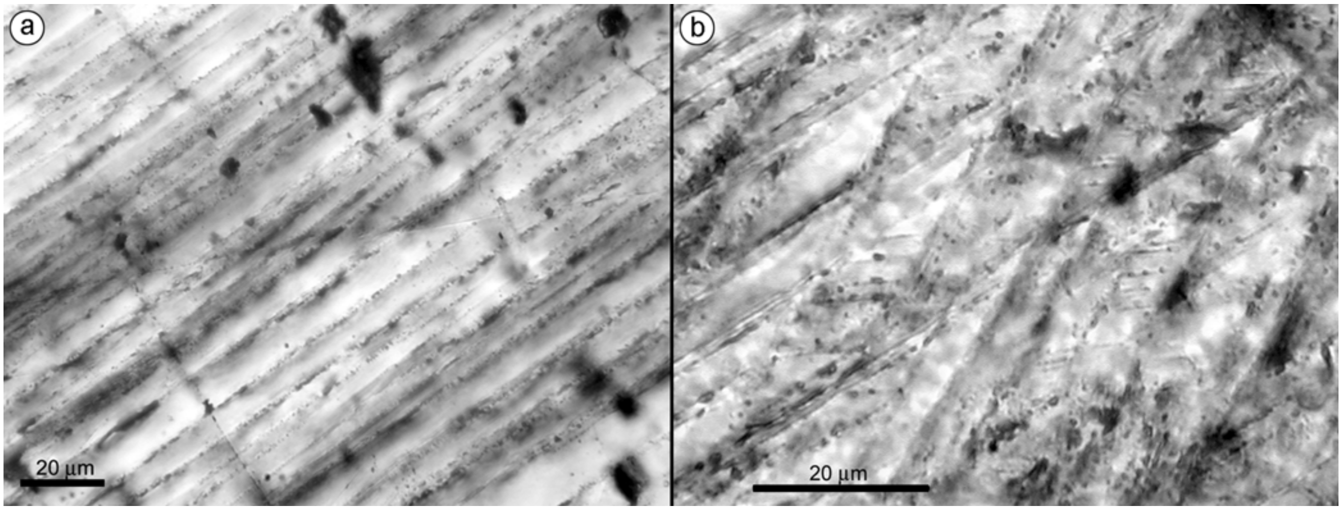

Fig. 5. Optical micrographs in polarized light show shocked quartz grains with PDFs from the Ries impact crater, Germany. a) Quartz grain showing one set of parallel PDFs. b) Quartz grain showing three sets of PDFs. Two sets are continuous and well developed; one set is discontinuous (horizontal in the picture) and is decorated with fluid inclusions.

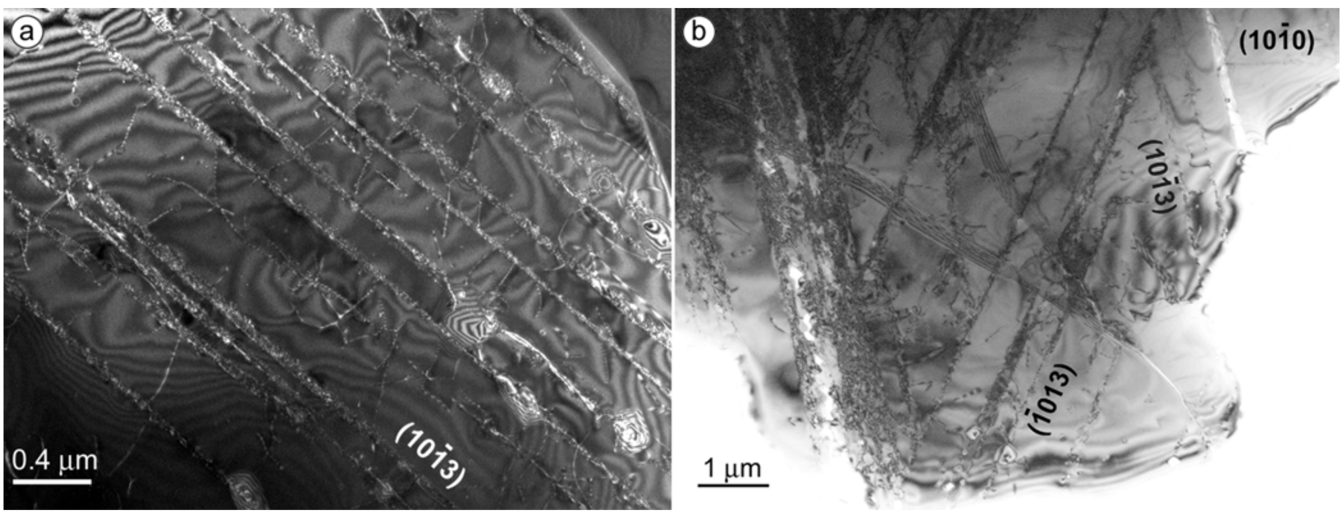

Fig. 6. TEM images of PDFs in shocked quartz grains. The PDFs were post-shock annealed and decorated with tiny dislocation loops and fluid inclusions. a) Dark field weak beam image ($g = 10\bar{1}1$) shows one single set of perfectly planar PDFs with orientation $(10\bar{1}3)$. Since there are no contrast changes across the PDFs, the orientation of the crystal lattice is uniform. b) Bright field image of three sets of PDFs with orientations $(10\bar{1}3)$, $(\bar{1}013)$, and $(10\bar{1}0)$.

numerous curved free dislocations indicates that both glide- and climb-controlled processes have been active during the deformation of samples. This coexistence of creep and recovery and the formation of deformation lamellae point to deformation in the so-called exponential creep regime, where the deformation behavior does not follow any more a power law of creep (McLaren 1991; Drury 1993).

To understand the development of the defect microstructure and, in particular, the formation of deformation lamellae in more detail, it is useful to discuss our observations in the context of previous extensive deformation experiments on quartz (see summaries of McLaren 1991; den Brok 1992; Doukhan 1995). These experiments have shown that dry quartz is practically undeformable and fails by fracturing, whereas small amounts of dissolved water lead to a drastic softening of quartz (so-called “hydrolytic weakening” [McLaren et al. 1989]). Thereby, the actual concentration and dispersion of water in the quartz structure plays an important role in the evolution of the deformation microstructure (Cordier and Doukhan 1989, 1995; Doukhan 1995). Quartz supersaturated in water (>180 ppm) precipitates numerous water bubbles, which subsequently grow with time and are the sources for homogeneous, pervasive emission and climb of dislocations. If quartz is, however, undersaturated in water, precipitation does not occur. Dislocation nucleation is heterogeneous along slip bands and climb of dislocations is strongly suppressed.

Deformation lamellae have only been found in our quartz crystals that were deformed to low strains (Table 1), suggesting that they form in an early stage of deformation when dislocations are heterogeneously emitted in slip bands and the quartz crystals are still undersaturated in water. The presence of homogeneously distributed free dislocations within subgrains and their configuration in the form of junctions point, however, to a change in the deformation mechanism. As the deformation experiments proceeded, more and more of the available water was probably incorporated into the quartz crystals and water precipitated as bubbles, from which dislocations were then homogeneously and pervasively emitted. In samples deformed to large strains, recovery was very efficient and defect microstructures are therefore strongly evolved such that initially formed deformation lamellae can completely vanish.

This model of formation of deformation lamellae by initial dislocation glide in bands and dynamical recovery allows to also understand the subbasal orientations and broad angular variation of lamella orientations. Deformation lamellae are most abundant in quartz crystals deformed with the *c* axis at 45° to the compression axis (GRZ16, GRZ28), because in this orientation it is easiest to activate the energetically favorable 1/3<11$\bar{2}$0> dislocations in the (0001) plane. While dislocation glide drives these dislocations along the (0001) plane, the synkinematic or subsequent climb of dislocations results in a movement out of the (0001) slip plane and an arrangement of dislocations into subgrain walls that are rotated away from the basal plane. The degree of rotation is thereby controlled by the relative speeds of glide and climb. This explanation for the subbasal orientation of lamellae is supported by the observation that subgrain walls usually consist of well-organized, straight dislocations. Networks of dislocations are not observed because only a single set of *a* dislocations has been emitted in the basal plane. A similar model for the formation of deformation lamellae was presented by Drury (1993) to explain the formation of subgrain walls containing a network of dislocations in two slip planes.

Distinction between Deformation Lamellae and Planar Deformation Features

In the context of recent discussions on the origin of planar features in quartz from suspected impact structures and boundary layers (e.g., Retallack et al. 1998; Becker et al. 2004; Langenhorst et al. 2005), it might be useful to finally recall here the fundamental difference between deformation lamellae and shock-induced PDFs. A large number of TEM studies have shown that fresh PDFs represent planar and thin glass lamellae with a composition identical to that of the host crystal (e.g., Gratz et al. 1992; Langenhorst 1994). Post-shock annealing in natural impact formations results in the recrystallization of glass lamellae, the formation of tiny dislocation loops, and precipitation of water bubbles (Grieve et al. 1996; Langenhorst and Deutsch 1998). PDFs are therefore often decorated with fluid inclusions, but this does neither change their orientation nor their planarity. The PDFs that are observed within the analyzed shocked quartz grains from the Ries crater are of this "decorated" type.

At the TEM scale, there are thus abundant criteria to distinguish PDFs from deformation lamellae; they can be summarized as follows: (i) PDFs are perfectly planar instead of slightly curved, (ii) they strictly form parallel to defined (mostly rhombohedral) crystallographic planes, (iii) their spacing is usually <1 μm instead of 2–4 μm, (iv) they do not induce a misorientation within the crystal and, thus, are not subgrain walls or dislocation bands, and (v) the density of free dislocations is low compared to quartz with deformation lamellae. Although the resolution of the optical microscope does not allow to see the detailed defect microstructure, most of the listed characteristics can also be recognized at the optical scale. Therefore, TEM study is not necessarily demanded to identify the origin of planar features (Lyons et al. 1993) but may be recommendable in cases of suspected impact structures with samples that experienced strong thermal overprint (Leroux et al. 1994; Joreau et al. 1997). A careful optical analysis of planar features, the precise measurement of orientations using the universal stage (Langenhorst 2002), the inspection of cogenetic minerals, and the geologic setting are usually sufficient criteria to distinguish PDFs from deformation lamellae (Reimold 1994).

Acknowledgments–MV is grateful for a Marie-Curie research grant provided by the Bayerisches Geoinstitut, University of Bayreuth (IHP program, HPMT-CT-2001-00231, to D. Rubie), and for financial support by ETH project 0-20907-01. We are indebted to B. den Brok for fruitful discussions and to W. U. Reimold and an anonymous reviewer for the constructive reviews.

Editorial Handling—Dr. Wolf Uwe Reimold

REFERENCES

Becke F. 1893. Petrographische Studien am Tonalit der Riesenferner. *Tschermak's Mineralogische und Petrographische Mitteilungen* 13:79–464.

Böhm A. 1882. Ueber die Gesteine des Wechsels. *Mineralogische und Petrographische Mitteilungen* 4:197–214.

Becker L., Poreda R. J., Basu A. R., Pope K. O., Harrison T. M., Nicholson C., and Iasky R. 2004. Bedout: A possible end-Permian impact crater offshore of Northwestern Australia. *Science* 304:1469–1476.

Blenkinsop T. G. and Drury M. R. 1988. Stress estimates and fault history from quartz microstructures. *Journal of Structural Geology* 10:673–684.

Christie J. M. and Ardell A. J. 1974. Substructures of deformation lamellae in quartz. *Geology* 2:405–408.

Christie J. M. and Ardell A. J. 1976. Deformation structures in minerals. In *Electron microscopy in mineralogy,* edited by Wenk H.-R. Berlin: Springer. pp. 374–403.

Christie J. M. and Raleigh C. B. 1959. The origin of deformation lamellae in quartz. *American Journal of Science* 257:385–407.

Cordier P. and Doukhan J. C. 1989. Water in quartz, solubility and influence on ductility. *European Journal of Mineralogy* 1:221–237.

Cordier P. and Doukhan J. C. 1995. Plasticity and dissociation of dislocations in water-poor quartz. *Philosophical Magazine A* 72: 497–514.

Cordier P., Vrána S., and Doukhan J. C. 1994. Shock metamorphism in quartz at Sevetin and Susice (Bohemia)? A TEM investigation. *Meteoritics* 29:98–99.

Doukhan J. C. 1995. Lattice defects and mechanical behavior of quartz SiO_2. *Journal de Physique III France* 5: 1809–1932.

Den Brok B. 1992. An experimental investigation into the effect of water on the flow of quartzite. *Geologica Ultraiectina* 95.

Drury M. R. 1993. Deformation lamellae in metals and minerals. In *Defects and processes in the solid state: Geoscience applications*, edited by Boland J. N. and Fitz Gerald J. D. Amsterdam: Elsevier. pp. 195–212.

French B. M. 1998. *Traces of catastrophe—A handbook of shock-metamorphic effects in terrestrial meteorite impact structures.* LPI Contribution #954. Houston, Texas: Lunar and Planetary Institute.

Gratz A. J., Nellis W. J., Christie J. M., Brocious W., Swegle J., and Cordier P. 1992. Shock metamorphism of quartz with initial temperatures −170 to 1000 °C. *Physics and Chemistry of Minerals* 19:267–288.

Grieve R. A.F., Langenhorst F., and Stöffler D. 1996. Shock metamorphism of quartz in nature and experiment: II. Significance in geoscience. *Meteoritics & Planetary Science* 31: 6–35.

Goltrant O., Cordier P., and Doukhan J.-C. 1991. Planar deformation features in shocked quartz—A transmission electron microscopy investigation. *Earth and Planetary Science Letters* 106:103–115.

Goltrant O., Leroux H., Doukhan J. C., and Cordier P. 1992. Formation mechanisms of planar deformation features in naturally shocked quartz. *Physics of the Earth and Planetary Interiors* 74:219–240.

Joreau P., Reimold W. U., Robb L. J., and Doukhan J. C. 1997. A TEM study of deformed quartz grains from volcaniclastic sediments associated with the Bushveld complex, South Africa. *European Journal of Mineralogy* 9:393–401.

Langenhorst F. 1994. Shock experiments on pre-heated α- and β-quartz: II. X-ray and TEM investigations. *Earth and Planetary Science Letters* 128:683–698.

Langenhorst F. 2002. Shock metamorphism of some minerals: Basic introduction and microstructural observations. *Bulletin of the Czech Geological Survey* 77:265–282.

Langenhorst F. and Deutsch A. 1994. Shock experiments on pre-heated α- and β-quartz: I. Optical and density data. *Earth and Planetary Science Letters* 125:407–420.

Langenhorst F. and Deutsch A. 1996. The Azuara and Rubielos structures, Spain: Twin impact craters or alpine thrust systems? TEM investigations on deformed quartz disprove shock origin (abstract). 27th Lunar and Planetary Science Conference. pp. 725–726.

Langenhorst F., and Deutsch A. 1998. Minerals in terrestrial impact structures and their characteristic features. In *Advanced mineralogy*, vol. 3, edited by Marfunin A.S. Berlin: Springer pp. 95–119.

Langenhorst F., Deutsch A., Hornemann U., and Stöffler D. 1992. Effect of temperature on shock metamorphism of single crystal quartz. *Nature* 356:507–509.

Langenhorst F., Kyte F. T., and Retallak G. J. 2005. Reexamination of quartz grains from the Permian-Triassic boundary section at Graphite Peak, Antarctica (abstract #2358). 36th Lunar and Planetary Science Conference. CD-ROM.

Leroux H., Reimold W. U., and Doukhan J. C. 1994. A TEM investigation of shock metamorphism in quartz from the Vredefort dome, South Africa. *Tectonophysics* 230:223–239.

Leroux H., Warme J. E., and Doukhan J.-C. 1995. Shocked quartz in the Alamo breccia, southern Nevada: Evidence for a Devonian impact event. *Geology* 23:1003–1006.

Lyons J. B., Officer C. B., Borella P. E., and Lahodynsky R. 1993. Planar lamellar substructures in quartz. *Earth and Planetary Science Letters* 119:431–440.

McLaren A. C. 1991. *Transmission electron microscopy of minerals and rocks*. Cambridge: Cambridge University Press. 397 p.

McLaren A. C., Turner R. G., Boland J. N., and Hobbs B. E. 1970. Dislocation structure of lamellae in synthetic quartz. *Contributions to Mineralogy and Petrology* 29:104–115.

McLaren A. C. and Hobbs B. E. 1972. Transmission electron microscope investigation of some naturally deformed quartzites. In *Flow and fracture of rocks*, edited by Heard H. C., Borg I. Y., Carter N. L., and Raleigh C. B. Washington, D.C.: American Geophysical Union. pp. 55–66.

McLaren A. C., Fitzgerald J. D., and Gerretsen J. 1989. Dislocation nucleation and multiplication in synthetic quartz: Relevance to water weakening. *Physics and Chemistry of Minerals* 16:465–482.

Mossman D. J., Grantham R. G., and Langenhorst F. 1998. A search for shocked quartz at the Triassic-Jurassic boundary in the Fundy and Newark basins of the Newark Supergroup. *Canadian Journal of Earth Sciences* 35:101–109.

Reimold W. U. 1994. Comment on "Planar lamellar substructures in quartz" by Lyons et al. (1993). *Earth and Planetary Science Letters* 125:473–477.

Retallack G. J., Seyedolali A., Krull E. S., Holser W. T., Ambers C. P., and Kyte F. T. 1998. Search for evidence of impact at the Permian-Triassic boundary in Antarctica and Australia. *Geology* 25:979–982.

Sharp T. G., El Goresy A., Wopenka B., and Chen M. 1999. A post-stishovite SiO_2 polymorph in the meteorite Shergotty: Implications for impact events. *Science* 284:1511–1513.

Stöffler D. 1971. Progressive metamorphism and classification of shocked and brecciated crystalline rocks at impact craters. *Journal of Geophysical Research* 76:5541–5551.

Stöffler D. and Ostertag R. 1983. The Ries impact crater. *Fortschritte der Mineralogie* 61:71–116.

Stöffler D. and Langenhorst F. 1994. Shock metamorphism of quartz in nature and experiment: I. Basic observation and theory. *Meteoritics* 29:155–181.

Tullis J. and Tullis T. E. 1986. Experimental rock deformation techniques. In *Mineral and rock deformation: Laboratory studies*, edited by Hobbs B. E. and Heard H. C. Washington, D.C.: American Geophysical Union. pp. 297–324.

White S. H. 1973. Deformation lamellae in naturally deformed quartz. *Nature Physical Science* 245: 26–28.